

Size of Bubbles and Gas Holdup in Bubble Columns

Toshiro MIYAHARA* and Teruo TAKAHASHI*

(Received January 16, 1986)

SYNOPSIS

Bubble columns are extensively used in the chemical industry. This paper evaluates the present state of the art on the size of bubbles from a sieve plate and gas holdup, mainly on the basis of the results of the authors, including previous ones.

The size of bubbles formed from a sieve plate has an insignificant effect of chamber volume, and gas holdup shows some different behavior, depending on the hole diameter to liquid depth.

INTRODUCTION

Bubble columns are widely used in chemical process industries as contactors for carrying out gas-liquid or gas-liquid-solid reactions such as oxidations, hydrogenations, chlorination, coal liquefaction, aerobic fermentations, etc., because of their simplicity of construction and their high volumetric coefficient, leading to a large number of publications. Therefore, we have come across a considerable number of relevant papers on the size of bubbles and gas holdup available to the design and the operation of bubble columns. However, there remains uncertainties in the correlating equations because of different results of each investigator. The authors have also investigated these properties.

* Department of Industrial Chemistry

This paper reveals the present state of the art on the size of bubbles and gas holdup from point of view of the results of the authors⁽¹²⁻¹⁴⁾ together with previous ones.

1. EXPERIMENTAL APPARATUS AND PROCEDURE

The experimental apparatus is shown diagrammatically in Figure 1.

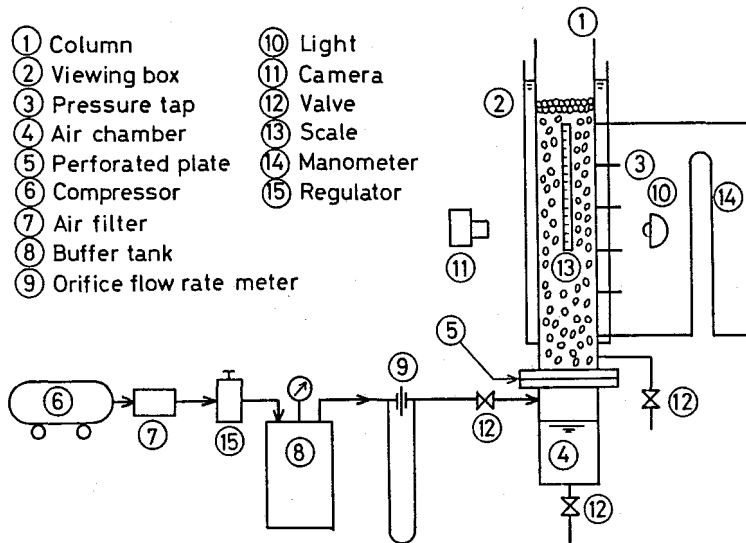


Fig. 1 Schematic diagram of experimental apparatus

Three different transparent acrylic-resin columns 1 were used, with internal diameters of 5, 10 and 15 cm. Most of the sieve plates 5, shown in Table 1, which show plate P-1 - P-22, were made of brass, with holes arranged in the form of equilateral triangles, except for plate P-4, for which the arrangement was square. To examine the effect of plate materials, polyethylene, polyvinylchloride, acrylic resin and teflon sieve plates, which are plate P-23 - P-31, were used; the column diameter was 5 cm, all the sieve plates employed for the purpose had the number of holes of 15 and the pitch of 1 cm, and distilled water was used as liquid. Details of the geometry are given in Table 1. Only teflon plate has a characteristic of non-wettability, showing a contact angle of liquid on a plate of more than 90 degrees. The liquids used for most of the tests were distilled water and

Table 1 Details of plates employed

Plate	d_o [m]	m [-]	P [m]	l [m]	P/d_o [-]	D_T [m]	Material	Contact angle [rad]
P-1	0.0005	19	0.01	0.001	20	0.05	Brass	0.52
P-2	0.001	19	0.01	0.001	10	0.05	Brass	0.52
P-3	0.0005	37	0.007	0.001	14	0.05	Brass	0.52
P-4	0.0005	37	0.002	0.001	4	0.05	Brass	0.52
P-5	0.0005	19	0.001	0.001	2	0.05	Brass	0.52
P-6	0.0005	19	0.002	0.001	4	0.05	Brass	0.52
P-7	0.0005	19	0.003	0.001	6	0.05	Brass	0.52
P-8	0.0005	19	0.004	0.001	8	0.05	Brass	0.52
P-9	0.0008	19	0.003	0.001	3.75	0.05	Brass	0.52
P-10	0.0005	85	0.01	0.001	20	0.1	Brass	0.52
P-11	0.0013	84	0.01	0.0008	7.69	0.1	Brass	0.52
P-12	0.0018	84	0.01	0.0008	5.56	0.1	Brass	0.52
P-13	0.001	1	-	0.001	-	0.15	Brass	0.52
P-14	0.001	2	0.01	0.001	10	0.15	Brass	0.52
P-15	0.001	3	0.01	0.001	10	0.15	Brass	0.52
P-16	0.001	5	0.01	0.001	10	0.15	Brass	0.52
P-17	0.001	10	0.01	0.001	10	0.15	Brass	0.52
P-18	0.001	15	0.01	0.001	10	0.15	Brass	0.52
P-19	0.001	17	0.01	0.001	10	0.15	Brass	0.52
P-20	0.0005	10	0.01	0.001	20	0.15	Brass	0.52
P-21	0.0005	13	0.01	0.001	20	0.15	Brass	0.52
P-22	0.0005	17	0.01	0.001	20	0.15	Brass	0.52
P-23	0.0005	19	0.01	0.002	20	0.05	Polyethylene	1.22
P-24	0.0005	19	0.01	0.002	20	0.05	Polyvinylchloride	1.08
P-25	0.001	19	0.01	0.002	10	0.05	Polyvinylchloride	1.08
P-26	0.0015	19	0.01	0.002	6.67	0.05	Polyvinylchloride	1.08
P-27	0.0005	19	0.01	0.002	20	0.05	Acryl resin	0.87
P-28	0.0005	19	0.01	0.001	20	0.05	Teflon	1.66
P-29	0.0008	19	0.01	0.001	12.5	0.05	Teflon	1.66
P-30	0.0011	19	0.01	0.001	10	0.05	Teflon	1.66
P-31	0.0015	19	0.01	0.001	6.67	0.05	Teflon	1.66

ethanol. The liquid depth was 25-100 cm.

Photographs were taken of bubbles at intervals of approximately 5 cm along the column. The negatives were enlarged, and the major and minor axes of each bubble, assumed to be ellipsoidal, were measured. The volumetric mean bubble diameter was calculated from the expression

$$\bar{d}_{30} = \left(\frac{\sum 6V_b/\pi}{n} \right)^{1/3} \quad (1)$$

The number of bubbles was 40-100, a level of which is reliable for statistical purpose under the above experimental conditions⁽⁶⁾.

Since under these experimental conditions, there was no appreciable variation in the size of bubbles in the longitudinal direction along the column, bubbles were photographed at a position 40-45 cm above sieve plate, except when we were examining the effect of the number of holes. Then, the photographs were taken at a depth of 25 cm. Gas holdup was calculated by the usual static pressure method.

2. RESULTS AND DISCUSSION

2.1 Size of Bubbles Generated from a Sieve Plate

1) Effect of hole number

According to the previous work⁽¹⁵⁾, the size of bubbles formed at single orifice is influenced by the volume of gas chamber; the same is true of bubbles generated from a sieve plate. On the other hand, the report by Koide et al.⁽⁶⁾ suggested that the size of bubbles from sieve plate is independent of gas chamber volume. In an attempt to find out the effect of the number of holes on the relationship between bubble size and chamber volume, we examine the bubble size for three cases of the chamber number $N_c < 1$, $1 < N_c < 9$, $9 < N_c$ ⁽¹⁵⁾, the results being shown in Figure 2. As can be seen, the effect of gas-chamber volume is much weaker with increase of the number of holes, the critical point being around 15 in the region of column diameters of 5-15 cm as shown in Figure 3. This is probably due to the liquid flow around the bubble induced by bubble formation. Accordingly, our subsequent experiments were carried out using 15 or more holes.

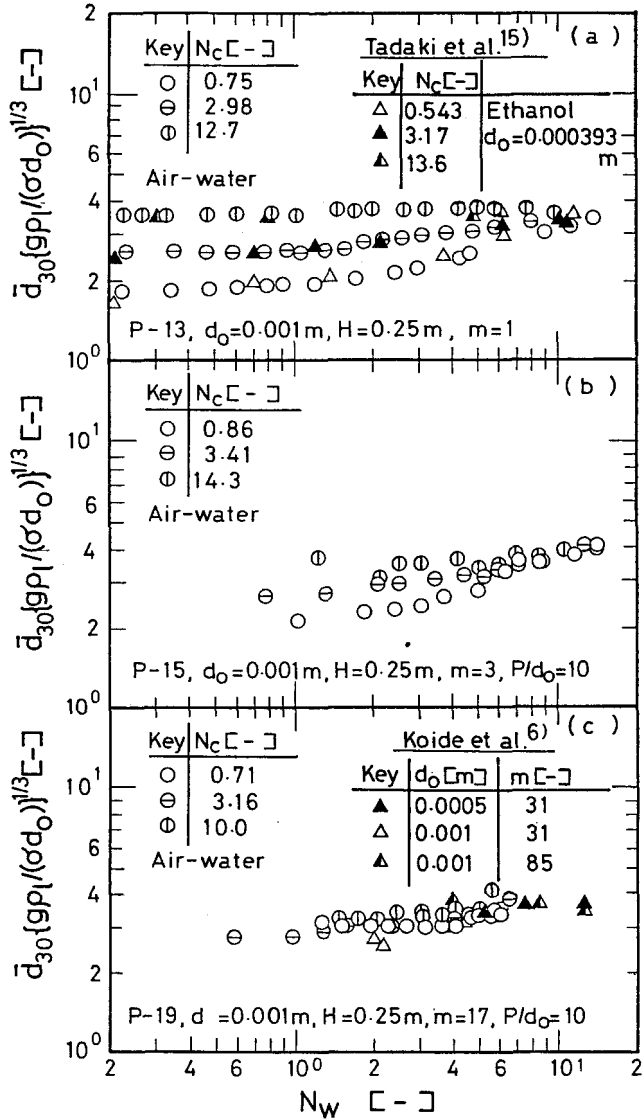


Fig. 2 Effect of chamber volume

2) Bubble size distribution

Figure 4 shows the volumetric mean diameter of bubbles for a low and a high value of pitch to hole diameter ratio p/d_0 . When P/d_0 is high, the volumetric mean diameter \bar{d}_{30} shows a minimum value, whereas it does not show for low values of P/d_0 . At gas velocity corresponding to the minimum bubble diameter, bubbles are generated from all the holes. The above result for low value of P/d_0 is due to the coalescence at the moment of bubble formation.

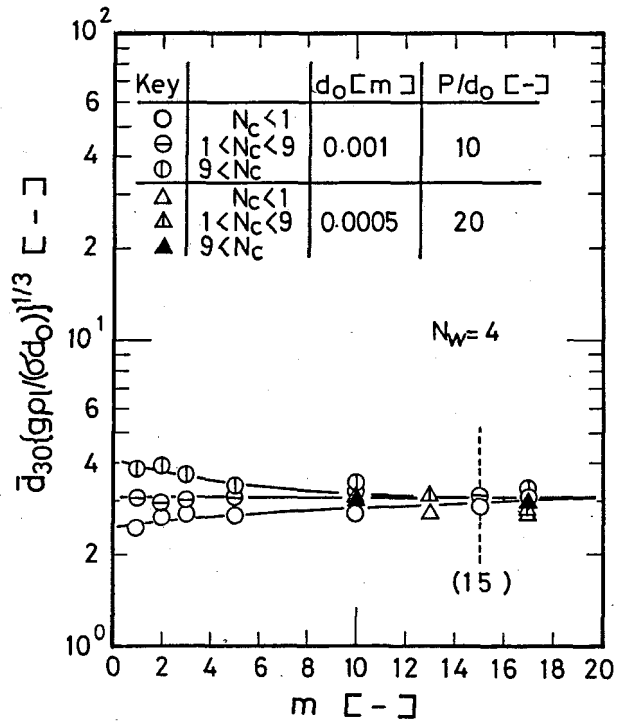


Fig. 3 Effect of number of holes

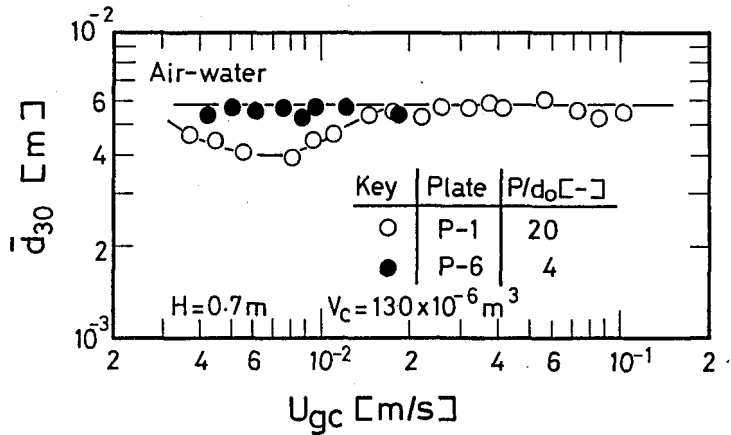


Fig. 4 Volumetric mean diameter of bubbles generated from sieve plate

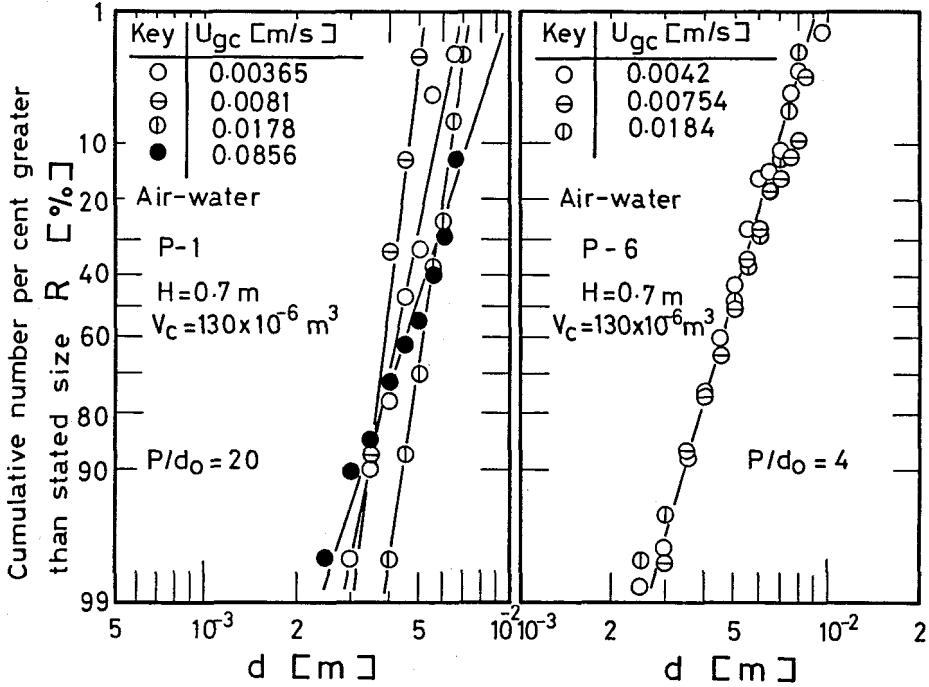


Fig. 5 Bubble size distribution

Figure 5 shows the bubble size distribution corresponding to Figure 4. The data are fitted well by a logarithmic normal probability distribution, the results agreeing with those of Tadaki et al.⁽¹⁵⁾, Towell et al.⁽¹⁷⁾ and Akita et al.⁽¹⁾. The distribution function can be expressed by

$$f(d, \bar{d}_g) = 1/(\sqrt{2\pi} \ln s) \exp[-\{\ln(d/\bar{d}_g)\}^2 / \{2(\ln s)^2\}] \quad (2)$$

Here,

$$\bar{d}_g = (d_1 \cdot d_2 \cdot d_3 \dots d_n)^{1/n} \quad (3)$$

$$s = \exp[\Sigma \{\ln(d/\bar{d}_g)\}^2 / n]^{1/2} \quad (4)$$

The size of bubbles for bubble columns is usually calculated as Sauter mean diameter \bar{d}_{32} . The Sauter mean diameter can be expressed on the basis of logarithmic normal probability distribution as

$$\bar{d}_{30}/\bar{d}_{32} = \exp\{-(\ln s)^2\} \quad (5)$$

Since s is close to unity as shown in Figure 6, we expect that \bar{d}_{30} is nearly equal to \bar{d}_{32} according to Eq.(5).

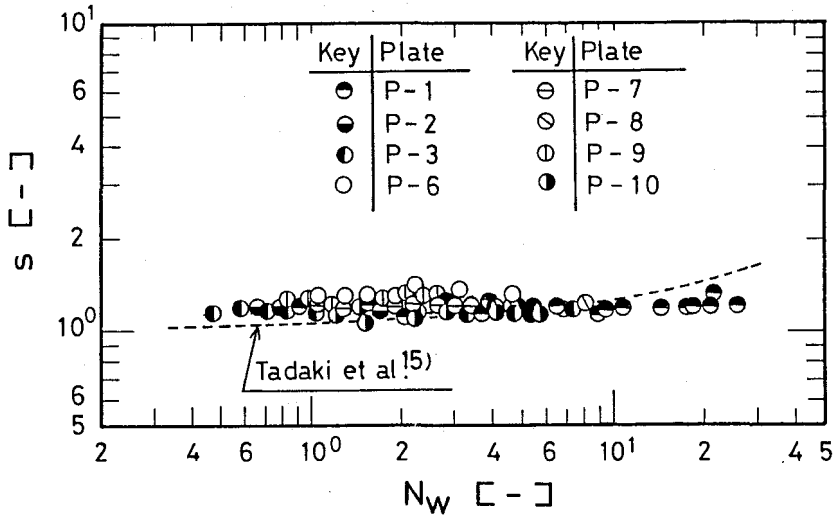


Fig. 6 Geometric standard deviation

3) Mean bubble diameter

Figure 7 shows the correlation for the dimensionless bubble diameter against the dimensionless parameter $N_w^{(15)}$ for $P/d_o > 8$, the experimental results and the correlation of Koide et al.⁽⁶⁾ also being shown. The solid line is

$$\bar{d}_{30} \{g\rho_l / (\sigma d_o)\}^{1/3} = f(N_w) \quad P/d_o > 8 \quad (6)$$

where

$$\begin{array}{ll} f(N_w) = 2.9 & N_w \leq 1 \\ f(N_w) = 2.9 N_w^{-0.188} & 1 < N_w \leq 2 \\ f(N_w) = 1.8 N_w^{0.5} & 2 < N_w \leq 4 \\ f(N_w) = 3.6 & 4 < N_w \end{array}$$

The dashed lines in the same graph are the correlation of Tadaki et al.⁽¹⁵⁾, the experimental results of this study being close to the result of Tadaki et al. for $N_w = 4$. The value of $N_w = 2$ corresponds to

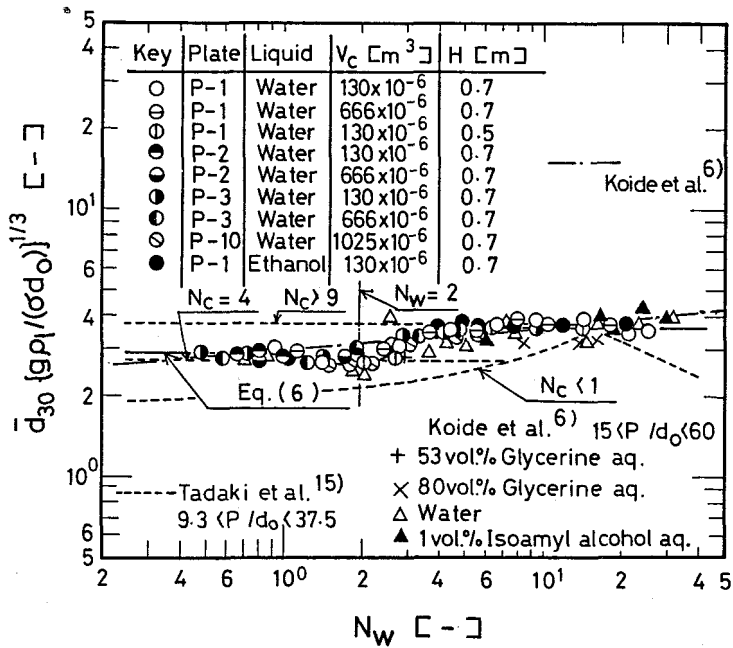


Fig. 7 Correlation of volumetric mean diameter of bubbles

the transitional points at which bubbles are generated from all the holes.

The following correlation has been found to be valid at low values of P/d₀ as shown in Figure 8.

$$\bar{d}_{30} \{g\rho_1 / (\sigma d_0)\}^{1/3} = 3.6 \quad P/d_0 < 8 \quad (7)$$

4) Effect of inorganic electrolytes

The addition of inorganic electrolytes to water has an insignificant effect on the size of bubbles generated from plates for P/d₀ > 8, whereas the bubble size for plates of P/d₀ < 8 shows complicated characteristics as dependent on concentrations and sorts of electrolyte, the bubble size being always smaller than that obtained by Eq.(7). The most likely reason is the inhibition of coalescence between adjacent bubbles at the plate due to the existence of inorganic electrolytes though P/d₀ is small.

Marrucci⁽⁹⁾ has recently proposed an idea for the thinning process of liquid film. This theory indicates that the bubble coalescence is hindered by the value of Cr_bk²/σ.

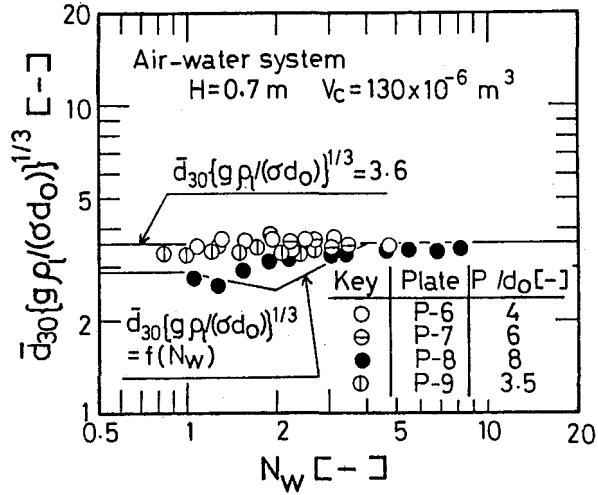


Fig. 8 Effect of P/d_o

Then, $Cr_b k^2 / \sigma$ represents the difficulty of bubble coalescence.

The correlation of the bubble size for the addition of inorganic electrolyte is illustrated in Figure 9 by α vs. $Cr_b k^2 / \sigma$; where α is

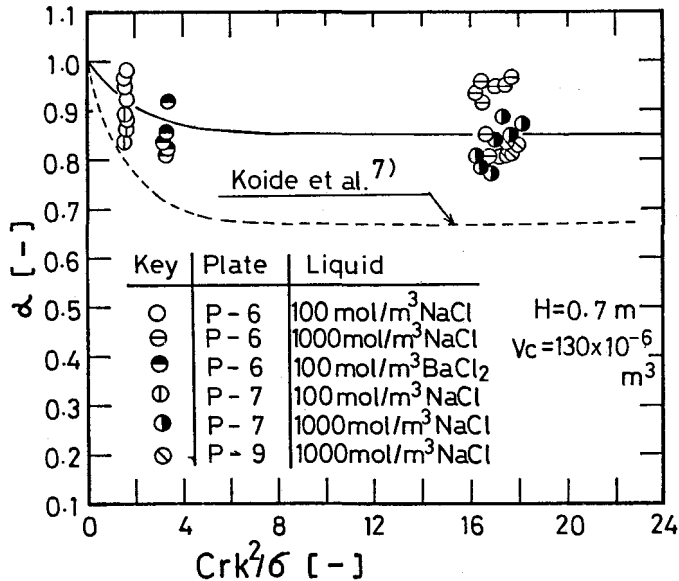


Fig. 9 Effect of inorganic electrolytes

the ratio of dimensionless bubble diameter in aqueous inorganic electrolytes to that in pure water.

The dashed line in this graph shows the result of bubble diameter for porous plate at the critical gas velocity below which bubble diameter does not depend on gas velocity, which was found by Koide et al. (7). It is clearly seen that the addition of inorganic electrolyte strongly affects the size of bubbles from porous plate.

5) Effect of plate materials

The size of bubbles from plates of non-wettable materials, whose characteristics depend on a contact angle of liquid on a plate of more than 90 degrees is independent of N_w for both $P/d_o > 8$ and $P/d_o < 8$ as shown in Figure 10.

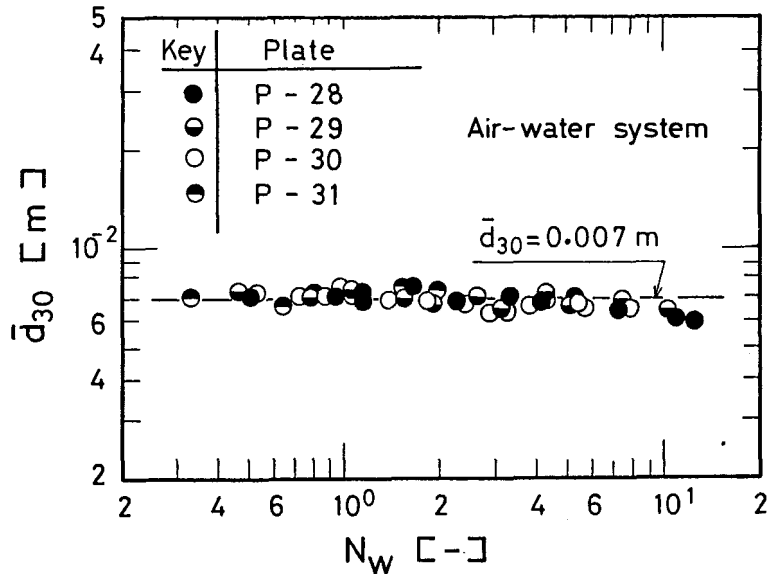


Fig. 10 Volumetric mean diameter of bubbles from various plates of non-wettable materials

The size of bubbles is about 7 mm, while the size distribution follows a normal probability distribution approximately when the standard deviation is given by

$$s'/d_o^{1/2} = 0.08 \quad (8)$$

as shown in Figure 11 above $N_w = 2$ at which bubbles are generated at all the holes.

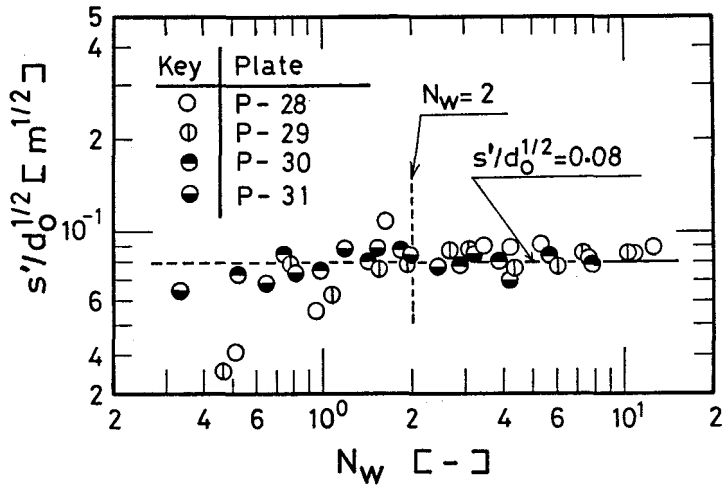


Fig. 11 Standard deviation

Table 2 Bubble size correlations in bubble column

Investigator	Correlation
Koide et al. ⁶⁾	$\bar{d}_{30} \{g\rho_l / (\sigma d_o)\}^{1/3} = 2.94 N_W^{0.071}$
Kumar et al. ⁸⁾	$\bar{d}_{32} \{\Delta\rho g / (\sigma d_o^2)\}^{1/4} = 1.56 Re_g^{0.058}$
	$\bar{d}_{32} \{\Delta\rho g / (\sigma d_o^2)\}^{1/4} = 0.32 Re_g^{0.425}$
	$\bar{d}_{32} \{\Delta\rho g / (\sigma d_o^2)\}^{1/4} = 100 Re_g^{-0.4}$
Akita et al. ¹⁾	$\bar{d}_{32} / D_T = 26 (g D_T^2 \rho_l / \sigma)^{-0.5}$
	$\times (U_{gc} / \sqrt{g D_T})^{-0.12} (g D_T^3 / \nu_l^2)^{-0.12}$

$\Delta\rho = \rho_l - \rho_g$

6) Previous bubble size correlations

A number of correlations for bubble size have been proposed, however, the scatter in reported data does not allow a single correlation. Some of the important correlations have been listed in Table 2.

Figure 12 shows the comparison among Eq.(6), the correlations shown in Table 2 and the present measurements.

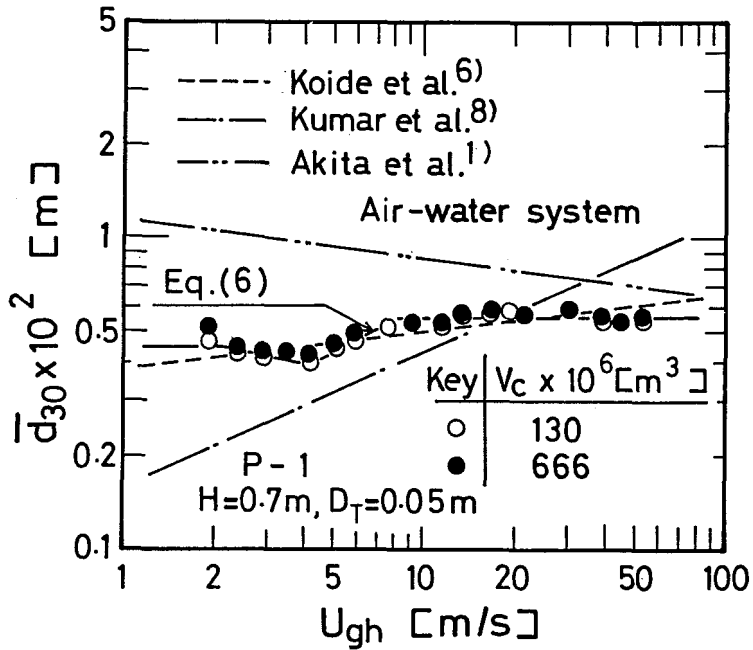


Fig. 12 Comparison between previous correlations and bubble size measurements

2.2 Gas Holdup in Bubble Column

1) Maximum gas holdup

Gas holdup in bubble columns increases with increasing gas velocity in the uniform bubbling regime, where bubbles rise independently with fairly uniform spacing between them, represents the maximum value and decreases in liquid circulation regime where the dynamic interaction of gross circulation and large bubbles becomes frequent and violent.

The maximum gas holdup is given for air-water system by the following equation⁽¹⁸⁾

$$(1 - \psi)_{\max} = 0.0083 \{ mP / (d_o D_T^2) \}^{0.29} \quad (9)$$

The critical superficial gas velocity which is defined as the velocity at the point of incipient regular circulation, where a transition from bubble to turbulent circulation flow occurs, depends on clear liquid height under a uniform stable gas distribution and is given by⁽¹⁰⁾

to this case, i.e., the long constant gas holdup region.

Now, the gas holdup in shallow liquid is correlated well with the Froude number based on liquid depth⁽¹⁶⁾. The gas-to-liquid holdup ratio in a deep liquid of 0.3 m to 1 m depth is presented in Figure 14 in terms with $(1-\Psi)/\Psi$ against Fr. The dashed lines are given by the following equations⁽¹⁶⁾

$$(1 - \Psi)/\Psi = 6.5\sqrt{Fr} \quad Fr < 8.5 \times 10^{-4} \quad (12)$$

$$(1 - \Psi)/\Psi = 2^3\sqrt{Fr} \quad 8.5 \times 10^{-4} < Fr < 1 \quad (13)$$

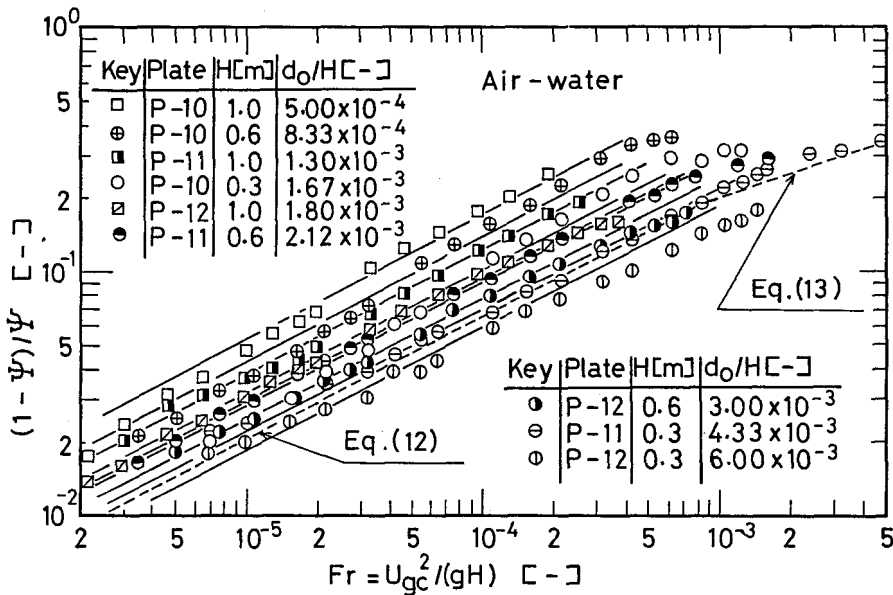


Fig. 14 Gas liquid holdup ratio versus Froude number

From this chart, gas holdup is satisfactory agreement with Eq.(12) for large d_0/H , whereas for small d_0/H it is larger than that of Eq.(12) and d_0/H does not affect gas holdup for large Froude numbers. When d_0/H is less than about 3×10^{-3} , gas holdup is independent of liquid depth. For this reason, it is presumed that liquid depth usually does not affect the gas holdup in bubble column.

Figure 15 shows the correlation of gas holdup in terms of $(1-\Psi)/\Psi$ against $Fr' (=U_{gc}^2/(gd_0))$ for $d_0/H < 3 \times 10^{-3}$. From this figure, the following empirical equation is obtained

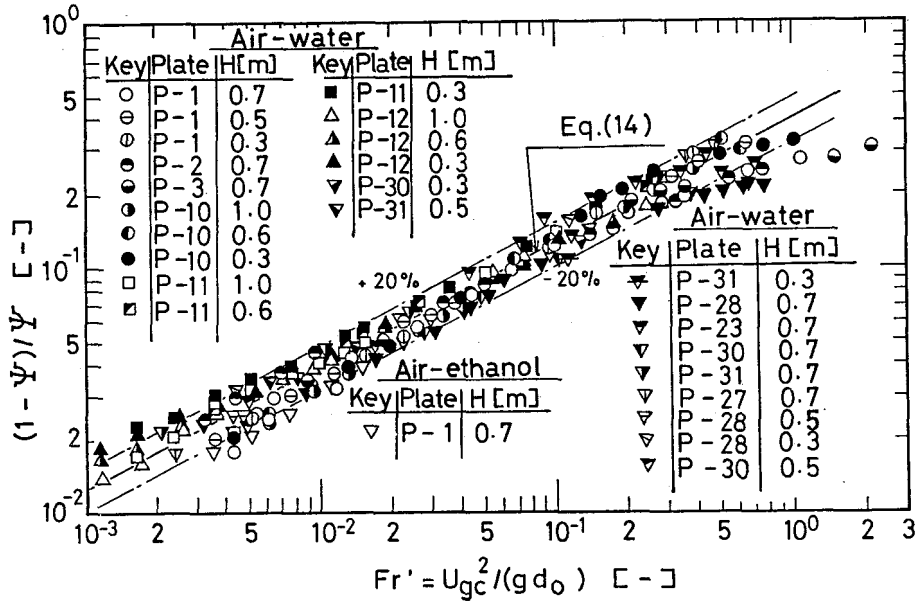


Fig. 15 Correlation of gas holdup

$$(1 - \Psi)/\Psi = 0.4\sqrt{Fr'} \quad Fr' = U_{gc}^2 / (gd_o), \quad d_o/H < 3 \times 10^{-3}$$

$$(1 - \Psi) < (1 - \Psi)_{\max} \quad (14)$$

It seems that $(1-\Psi)/\Psi$ in $d_o/H > 3 \times 10^{-3}$ or turbulent circulation flow regime could be estimated by Eqs. (12) and (13).

4) Previous gas holdup correlations

Some previously important correlations for gas holdup in bubble columns having a sieve plate are shown in Table 3.

Figure 16 shows the comparison among Eq. (14), the correlations in Table 3 and the present measurements.

CONCLUDING REMARKS

The size distribution of bubbles formed from a sieve plate may follow a logarithmic normal probability distribution when the geometric standard deviation is close to unity, whereas the size distribution of bubbles from a sieve plate of non-wettable material, being independent of the plate geometry, follows a normal probability

Table 3 Holdup correlations in bubble column

Investigator	Correlation
Hughmark ³⁾	$(1-\psi) = [2 + (0.35/U_{gc}) \{ (\rho_l/\rho_w) (\sigma/\sigma_w) \}^{1/3}]^{-1}$
Gestrich et al. ²⁾	$(1-\psi) = 0.89 (H/D_T)^{0.036} (-15.7 + \log K) (d_b/D_T)^{0.3}$ $\times \{ (U_{gc}^2 / (g d_b)) \}^{0.025} (2.6 + \log K) K^{0.047} - 0.05$ $K = \rho_l \sigma^3 / (g \mu_l^4), d_b = 0.003 \text{ m}$
Kumar et al. ⁸⁾	$(1-\psi) = 0.728 U^{*2} - 0.485 U^{*2} + 0.0975 U^{*3}$ $U^* = U_{gc} \{ \rho_l^2 / (\sigma \Delta \rho g) \}^{1/4}, \Delta \rho = \rho_l - \rho_g$
Mersmann ⁹⁾	$(1-\psi) / \psi^4 = 0.14 U_{gc} \{ \rho_l^2 / (\sigma \Delta \rho g) \}^{1/4}$ $\times \{ \rho_l^2 \sigma^3 / (\mu_l^4 \Delta \rho g) \}^{1/24} (\rho_l / \rho_g)^{5/72}$ $\times (\rho_l / \Delta \rho)^{1/3} \quad \Delta \rho = \rho_l - \rho_g$
Kato et al. ^{4,5)}	$(1-\psi) = U_{gc} / v_b$ $v_b = 0.31 + 0.4 U_{gc}^{0.8} (1 - e^\gamma)$ $\beta = 4.5 - 3.5 e^{-25.5 D_T^{1.3}}$ $\gamma = -716 U_{gc}^{1.8} / \beta$

distribution.

The gas holdup on a sieve plate is different above and below a value of d_o/H of 3×10^{-3} . The gas holdup in bubble column is well correlated with the Froude number based on hole diameter, as independent of liquid depth.

NOMENCLATURE

A = Hamaker constant

[J]

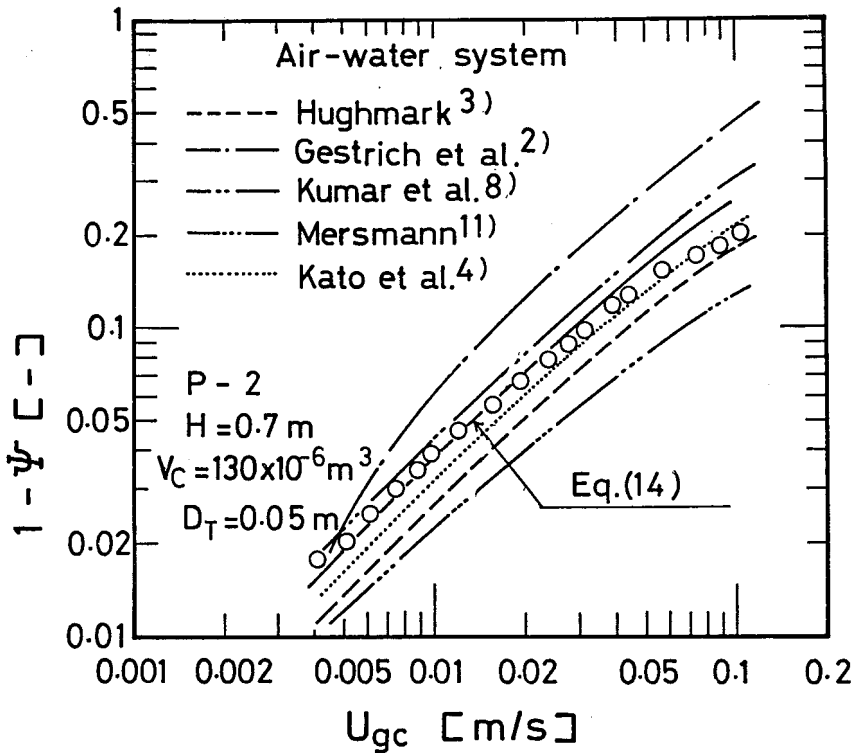


Fig. 16 Comparison between previous correlations and holdup measurements

$$C = \frac{2c_1}{nRT} \left(\frac{d\sigma}{dc_1} \right)^2 \frac{1}{1 + (d \ln f_1 / d \ln c_1)} \frac{1}{1 + (x_1 v_1 / x_2 v_2)} \quad [\text{N}]$$

c_1 = concentration of component 1 [mol / m³]

$Cr_b k^2 / \sigma$ = parameter of bubble coalescence proposed by Marrucci [-]

D_T = column diameter [m]

d = bubble diameter [m]

\bar{d}_{30} = volumetric mean diameter of bubbles [m]

\bar{d}_{32} = Sauter mean diameter [m]

\bar{d}_g = geometric mean diameter [m]

d_o = hole diameter [m]

Fr = Froude number = $U_{gc}^2 / (gH)$ [-]

Fr_h = Froude number = $U_{gh}^2 / (gd_o)$ [-]

Fr' = Froude number = $U_{gc}^2 / (gd_o)$ [-]

f_1 = activity coefficient of component 1 [-]

g = gravitational acceleration [m/s²]

H	= liquid depth	[m]
l	= thickness	[m]
m	= hole number	[-]
k	= $\{(2\pi\sigma/(Ar_b))\}^{1/3}$	[1/m]
N_c	= chamber number = $4V_c(\rho_l - \rho_g)g/(\pi d_o^2 P_c)$	[-]
N_w	= $We/Fr_h^{0.5}$	[-]
P_c	= pressure in chamber	[Pa]
P	= pitch	[m]
R	= gas constant	[J.K ⁻¹ .mol ⁻¹]
n	= total number of moles of ions per mole of electrolyte	[-]
Re_g	= Reynolds number = $d_o U_{gh} \rho_g / \mu_g$	[-]
R_T	= column radius	[m]
r	= radial distance	[m]
r_b	= bubble radius	[m]
s	= standard deviation	[m]
s_g	= geometric standard deviation	[-]
U_{gh}	= hole velocity	[m/s]
U_{gc}	= superficial gas velocity	[m/s]
v_1, v_2	= molar volume of component 1 and 2	[m ³ /mol]
We	= Weber number = $\rho_l U_{gh}^2 / \sigma$	[-]
x_1, x_2	= mole fraction of component 1 and 2	[-]

Greek letters

α	= ratio of dimensionless bubble diameter in aqueous inorganic electrolytes to that in water	[-]
μ_g, μ_l	= viscosity of gas and liquid	[Pa.s]
ν_l	= kinematic viscosity = μ_l / ρ_l	[m ² /s]
ρ_g, ρ_l, ρ_w	= density of gas, liquid and water	[kg/m ³]
σ, σ_w	= surface tension of liquid and water	[N/m]
ϕ	= gas holdup	[-]
ϕ_c, ϕ_w	= gas holdup at center and wall	[-]
Ψ	= mean liquid holdup	[-]
ψ	= liquid holdup	[-]

REFERENCES

- (1) K. Akita and F. Yoshida: Ind. Eng. Chem., Process Design Develop., 13 (1974), 84.

- (2) W. Gestrich and W. Rahse: *Chemie-Ing-Tech.*, 47 (1975), 8.
- (3) G.A. Hughmark: *Ind. Eng. Chem., Process Design Develop.*, 6 (1967), 218.
- (4) Y. Kato and A. Nishiwaki: *Intern. Chem. Eng.*, 12 (1972), 182.
- (5) Y. Kato, M. Nishinaka and S. Morooka: *Kagaku Kogaku Ronbunshu*, 1 (1975), 530.
- (6) K. Koide, T. Hirahara and H. Kubota: *Kagaku Kogaku*, 30 (1966), 712.
- (7) K. Koide, T. Hayashi, M. Noro, Y. Takemura, N. Kawamata and H. Kubota: *J. Chem. Eng. Japan*, 5 (1972), 236.
- (8) A. Kumar, T.E. Degaleesan, G.S. Laddha and H.E. Hoelscher: *Can. J. Chem. Eng.*, 54 (1976), 503.
- (9) G. Marrucci: *Chem. Eng. Sci.*, 24 (1965), 975.
- (10) T. Maruyama, S. Yoshida and T. Mizushima: *J. Chem. Eng. Japan*, 14, (1981), 352.
- (11) A. Mersmann: *Ger. Chem. Eng.*, 1 (1978), 1.
- (12) T. Miyahara, Y. Matsuba and T. Takahashi: *Kagaku Kogaku Ronbunshu*, 8 (1982), 13.
- (13) T. Miyahara, S. Kaseno and T. Takahashi: *Kagaku Kogaku Ronbunshu*, 8 (1982), 643.
- (14) T. Miyahara, Y. Matsuba, S. Kaseno and T. Takahashi: *J. Chem. Eng. Japan*, 15 (1982), 391.
- (15) T. Tadaki and S. Maeda: *Kagaku Kogaku*, 27 (1963), 402.
- (16) T. Takahashi, T. Miyahara and K. Shimizu: *J. Chem. Eng. Japan*, 7 (1974), 75.
- (17) G.D. Towell, C.P. Strand and G.H. Ackerman: *AIChE-I. Chem. Eng. Symp. Series (London)*, No.10 (1965), 97.
- (18) F. Yamashita and H. Inoue: *J. Chem. Eng. Japan*, 8 (1975), 334.